IOPscience iopscience.iop.org

Home Search Collections Journals About Contact us My IOPscience

Ghost imaging and ghost diffraction with pseudo-thermal light generated by means of a programmable SLM

This content has been downloaded from IOPscience. Please scroll down to see the full text.

2011 J. Phys.: Conf. Ser. 274 012004

(http://iopscience.iop.org/1742-6596/274/1/012004)

View the table of contents for this issue, or go to the journal homepage for more

Download details:

IP Address: 157.92.4.4
This content was downloaded on 24/08/2015 at 15:39

Please note that terms and conditions apply.

Journal of Physics: Conference Series **274** (2011) 012004 doi:10.1088/1742-6596/274/1/012004

Ghost imaging and ghost diffraction with pseudo-thermal light generated by means of a programmable SLM

M G Capeluto[1], H Duisterwinkel[2], C T Schmiegelow[1], D Francisco[1], S Ledesma[1] and C Iemmi[1]

[1] Departamento de Física J.J.Giambiagi, Facultad de Ciencias Exactas y Naturales, Universidad de Buenos Aires, 1426 Buenos Aires, Argentina.

[2] University of Groningen, 9747 AG Groningen, The Netherlands

E-mail: iemmi@df.uba.ar

Abstract. Ghost imaging and ghost diffraction are techniques in which information about the object or about its diffraction pattern is extracted by measuring the correlation between a reference beam and a beam that passes through the object. Although first experiments were carried on by using entangled photons, it was demonstrated that this technique can be performed by splitting incoherent pseudo-thermal radiation such as that obtained with a laser passing through a moving diffuser. In this work we implemented the use of a programmable phase spatial light modulator (SLM) in order to replace the rotating ground glass. In this way the random phase distributions obtained from the moving diffuser can be emulated by displaying onto the SLM different realizations of a random function with uniform distribution. Based on the programmability of the modulator we have studied the influence of diverse parameters such as speckle size or phase distributions in the final image quality. We carry on the experiment for two different cases ghost imaging and far field ghost diffraction.

1. Introduction

Coincidence, or ghost imaging, is a technique in which the information about an unknown object is obtained by means of intensity correlation measurements. Usually the set-up involves two light beams that are sent through distinct paths, one of them travels along a test arm, in which the object is placed, and the other travels along a reference arm. Then, the information is recovered from the spatial correlation function between the two beams.

In the former experiments the two correlated optical fields were obtained from spontaneous parametric down conversion (SPDC) [1-4]. The reconstruction of the image was attributed to the non-local quantum correlations between the photon pairs. Subsequently it was discovered that these kind of experiences could be carried on by using a classical pseudo-thermal light source [5,6]. Recently it was experimentally implemented by means of a source of classically correlated beams which allows emulating the behaviour of entangled beams [7]. The source consists of a laser beam that impinges onto a rotating ground glass, then the emerging light, that has a thermal-like statistic, is divided by a beam splitter. The two outgoing beams have strong spatial correlation both in the near field and in the far field allowing a good reconstruction of the object image and of the object diffraction pattern. The only advantage of entanglement with respect to classical correlation lies in the better visibility of

Published under licence by IOP Publishing Ltd

information i.e. a better signal to noise ratio. A deep analysis and comparison of these two types of radiation is presented by Gatti *et. al.* in [8] and Bennink *et. al.* in [9]. In spite of these experiments, the nature of spatial correlations obtained with pesudo-thermal sources and whether they can be interpreted as classical intensity correlations [10] or as non-local quantum correlations [11] is still under discussion. In order to demonstrate that this phenomena is not a process arising from non-local two photon interference, Shapiro [12] describes a computational ghost imaging arrangement that uses a programmable spatial light modulator, to replace the rotating ground glass, and only one detector. On one hand, they use a random but deterministic modulation of the wavefront to illuminate the object and a single pixel detector to collect the light. On the other hand, knowing the random modulation, they compute the intensity distribution that would have travelled along the reference arm. Then they perform the correlation from processes deferred in time.

In this work we implement the use of a liquid crystal television display (LCTV) working in phase mode in order to produce optical beams which exhibit a high level of spatial correlation. As the modulators are entirely programmable different experimental parameters can be modified in order to improve the process. In particular we have analyzed the influence of the speckle size, the phase distribution and the convergence rate on the ghost image quality. In the next section we perform a brief description of the basic theory used along the experiments. The experimental set-up and the results obtained for both, ghost imaging and far field ghost diffraction, are presented in section 3. Finally section 4 contains the conclusions.

2. Ghost imaging and ghost diffraction schemes

A basic diagram of the set up used to perform correlated imaging is sketched in figure 1. The pseudo-thermal beam is divided by a beam splitter in two beams that exhibit a strong spatial correlation. The test arm includes de object and the light is measured by detector D_1 that, depends on the experiment, could be a point-like detector or a bucket detector. In any case it is possible to obtaingin information about the spatial distribution of the object. The light that travels along the reference arm is detected by an array of pixels D_2. Functions h_1 and h_2 are the impulse response that describe the optical paths of beams 1 and 2.

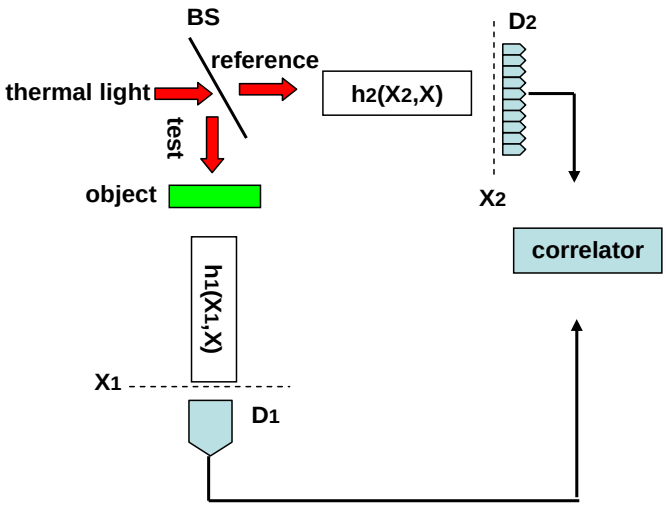

Figure 1: The pseudo-thermal light is divided at the beam splitter BS in two beams, the test arm which includes an object and the reference arm. Detector D_1 is either a point-like detector or a bucket detector, D_2 is an array of pixels detector

The object information is obtained from the spatial correlation of the intensities measured by detectors D_1 and D_2, and subtracting the background term

$$G(\vec{x}_1,\vec{x}_2)=\langle I_1(\vec{x}_1)\,I_2(\vec{x}_2)\rangle-\langle I_1(\vec{x}_1)\rangle\langle I_2(\vec{x}_2)\rangle \quad (1)$$

This expression can be written in terms of the reflection *r* and transmission *t* coefficients of the beam splitter and the impulse response functions h_1 and h_2 of the imaging systems, as was explained in detail in [8].

$$G(\vec{x}_1,\vec{x}_2)=|r\,t|^2\left|\int d\vec{x}_1^{\,\prime}d\vec{x}_2^{\,\prime}\;h_1^{*}(\vec{x}_1,\vec{x}_1^{\,\prime})\,h_2(\vec{x}_2,\vec{x}_2^{\,\prime})\Gamma_n(\vec{x}_1^{\,\prime},\vec{x}_2^{\,\prime})\right|^2 \tag{2}$$

where $\Gamma_n(\vec{x}_1^{\,\prime},\vec{x}_2^{\,\prime})$ is the second order correlation function of the speckle field at the object plane [7].

In our case the test arm is maintained fixed along the experiments, the object is placed in the front focal plane of a *f-f* system and the detector in the back focal plane. In this way the impulse response function that describe this arm is $h_1(\vec{x}_1,\vec{x}_1^{\,\prime})\,\alpha\exp(-i\vec{x}_1\cdot\vec{x}_1^{\,\prime}k/f)\,T(\vec{x}_1^{\,\prime})$ where $k=2\pi/\lambda$, λ is the wavelength and $T(\vec{x}_1^{\,\prime})$ is the object transmission.

In the ghost diffraction experiment the reference arm also has a *f-f* configuration, i.e. the detection plane where is situated the detector D_2 corresponds to the back focal plane of the optical system, consequently the impulse response function is $h_2(\vec{x}_2,\vec{x}_2^{\,\prime})\,\alpha\exp(-i\vec{x}_2\cdot\vec{x}_2^{\,\prime}k/f)$. As it was previously shown in [13] by scanning the test arm with a point-like detector and taking into account that the far field coherence length is wider than the detection area, equation (2) gives:

$$G(\vec{x}_1,\vec{x}_2)\,\alpha\left|\int d\vec{x}\,\tilde{T}^{*}(\vec{x}_1-\vec{x})\,\Gamma_f(\vec{x},\vec{x}_2)\,k/f\right|^2\alpha\left|\tilde{T}^{*}(\vec{x}_1-\vec{x})k/f\right|^2\left|\int d\vec{x}\,\Gamma_f(\vec{x},\vec{x}_2)\right|^2 \tag{3}$$

where $\tilde{T}(\vec{x})$ is the Fourier transform of $T(\vec{x})$, this is the Fraunhofer diffraction pattern of the object, and $\Gamma_f(\vec{x},\vec{x}^{\,\prime})$ is the far field speckle correlation function at the detection plane. The resolution in the ghost diffraction process will be limited by the far field coherence length. It should be pointed out that the proposed technique of using an array of pixels detector on the reference arm and scan the test arm with a point-like detector is equivalent to use an array of pixels on both arms and to perform the spatial correlation.

In the ghost image experiment the lens of the reference arm is changed by an optical system such that the detection plane is the conjugate of the object plane, being *m* the magnification between them. In this case the impulse response function that describes the arm 2 is $h_2(\vec{x}_2,\vec{x}_2)=m\,\delta(m\vec{x}_2+\vec{x}_2^{\,\prime})$. Thus equation (2) takes the form

$$G(\vec{x}_1,\vec{x}_2)\,\alpha\left|\int\; d\vec{x}_1^{\,\prime}\,T^{*}(\vec{x}_1^{\,\prime})\,\Gamma_n(\vec{x}_1^{\,\prime},-m\vec{x}_2)\exp(-i\vec{x}_1^{\,\prime}\cdot\vec{x}_1^{\,\prime}k/f)\right|^2 \tag{4}$$

If a sum over all the positions of D_1 is performed, which is equivalent to use a bucket detector, and considering that the smallest details in the object are larger than the near field coherence length, then it is possible to write

$$G(\vec{x}_2)\,\alpha\left|T(-m\vec{x}_2)\right|^2\left|\int\; d\vec{x}_1\;\Gamma_n(\vec{x}_1,-m\vec{x}_2)\right|^2 \tag{5}$$

This equation shows clearly that the information about the object transmission s recovered and that the resolution is limited by the speckle size on the object plane.

3. Experimental results

The experimental set-up used to perform ghost imaging and ghost diffraction is sketched in figure 2. We employed as light source the 457nm line, filtered from an Ar ion laser. The laser beam was

expanded with a microscope objective *E* and its size, when impinging onto the SLM, was controlled by means of lens L_1. The SLM used to provide the random phase modulation was composed of a Sony liquid crystal television panel *LCTV* model LCX012BL extracted from a commercial video-projector. This display, in combination with the adequate state of light polarization, provided by polarizers P_1, P_2 and the wave plates WP_1 and WP_2, allowed to reach a phase modulation near 2π under blue illumination [14]. This panel has VGA resolution (640 x 480 pixels) with square pixels with a side size of 34 μm and separated by a distance of 41.3 μm from center to center. As the LCTV is entirely programmable it is possible to display different phase distributions in order to emulate with fidelity the speckle distribution that would be obtained with a diffuser. We have found that the best results were obtained with a uniform random function. Moreover we have controlled the size of the areas with constant phase (i.e. 1x1, 2x2, 4x4 and 6x6 pixels) and its relationship with the illuminated area. In this way the speckle size and structure could be selected. A second lens L_2 and a diaphragm *D* were used in order to obtain an almost collimated speckle beam. The reference and object arms were obtained by means of a non-polarizing beam splitter cube *BS* which provides two nearly parallel beams with a high level of spatial correlation. Both arms illuminated two non overlapping portions of a *CCD* camera. The half corresponding to the reference arm acted always as a CCD, instead the half corresponding to the object arm acted either as a point-like detector or as a bucket detector, depending on the experiment. Lenses L_3 and L_4 were chosen in such a way that by removing lens L_3 the object plane and the CCD plane are in a configuration $f_4 - f_4$ (f_4 = 20 cm) for both the reference and the object arm. This situation allowed to obtain ghost diffraction. By inserting lens L_3 (f_3 = 17 cm) the reference arm changed to a configuration in which the object plane *O* and the CCD plane were conjugated so it was possible to obtain ghost imaging. In this last case the object arm remained in configuration $f_4 - f_4$ but this fact did not have any importance as just the total intensity (bucket detection) was performed.

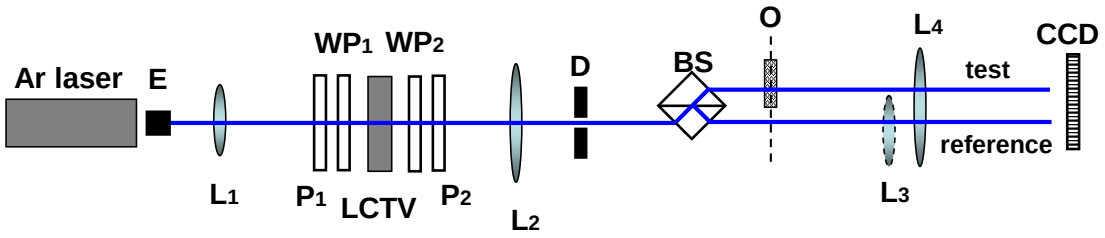

Figure 2: Experimental set-up. For ghost diffraction experiments lens L_3 is removed and both the test arm and the reference arm are in $f_4 - f_4$ configuration. For ghost imaging L_3 is inserted and the object plane is the conjugate of the CCD plane in the reference arm, the test arm remains unchanged.

3.1. Ghost imaging

In order to implement the ghost imaging process the experimental setup previously described was mounted. The light that travelled along the test arm, that contained the object, was collected by lens L_4 and the intensity distribution was detected as a whole by half of the CCD that acted like a bucket detector. This was performed by summing the intensity values along all the pixels belonging to that detection zone. Light travelling along the reference arm, did not pass through the object and was collected by the combination of lenses L_3 and L_4 which imaged the speckle distribution of the object plane onto the half of the CCD that acted like an array of detectors. By correlating this information according to equation (5) a ghost image was obtained. As an example figure 3 shows images when a single slit was used as object. Firstly the object was placed in the reference arm and illuminated with direct laser light (i.e. without a perturbing random phase media) in order to capture a regular image of

the slit (see figure 3a). Figure 3 b) shows a typical image obtained by moving the slit to the object arm and by displaying a random phase on the SLM. Figure 3c shows the ghost image reconstructed from 3.000 individual measurements and after applying the correlation process.

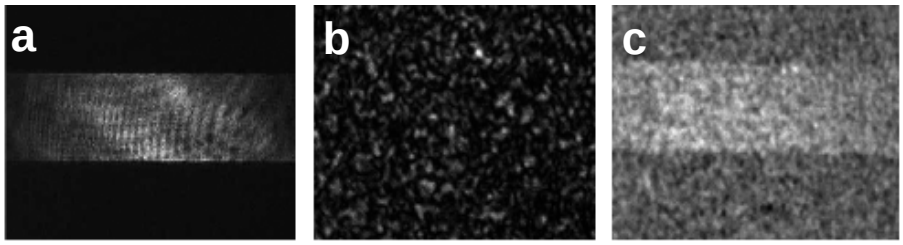

Figure 3: Ghost imaging. a) Image of the slit under direct laser illumination, b) an image of the reference arm when a random phase distribution is displayed onto the SLM, c) ghost image obtained after 3000 phase realizations

Let us to show the influence of the speckle coherence length on the spatial resolution of the ghost images. In order to see this effect we performed measurements using different spot sizes of the laser beam on the SLM. Figure 4 shows from top to bottom the result of increasing the spot size i.e. of a decreasing of the speckle sizes on the object plane. The images on the left show the speckles on the CCD for one measurement. The center images show the corresponding ghosts after 3000 phase realizations and the profiles on the right are the horizontal sums of the ghost images. By analyzing the slopes of these profiles its is clear that the images are sharper when the speckle size decreases.

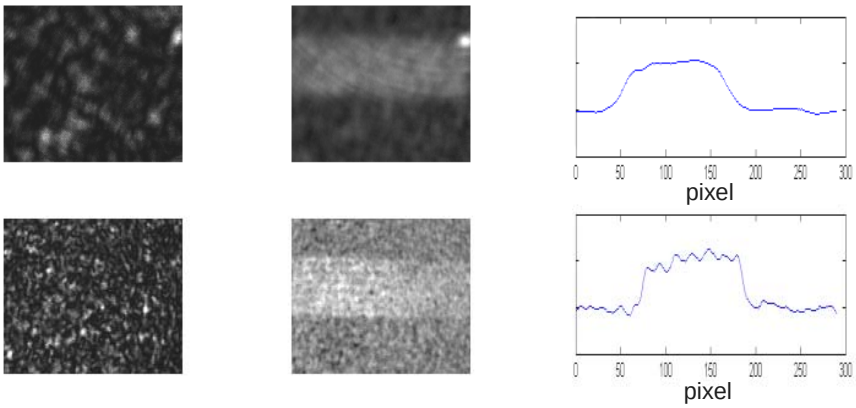

Figure 4: Image definition improvement by diminishing the speckle size

It is also of interest to analyze the effect of changing the size of the areas of constant phase on the LCTV. Let us to clarify this point: In order to obtain a speckle pattern we programmed a random uniform distribution of values to address different voltages to the pixels of the LCTV. The minimum area size with a constant phase value is 1x1 pixel, but this size can be changed. The constant phase areas on the LCD were changed from 1x1 pixel to 6x6 pixels. After each experiment a ghost image was obtained. Figure 5 shows, from left to right, the speckles on the CCD for one measurement, the ghost images obtained after 5000 realizations and the profile of the ghost images calculated from the sum of the pixels values in the horizontal direction. On the top the constant phase area occupies 6x6 pixels, on the bottom the area is of 1x1 pixel.

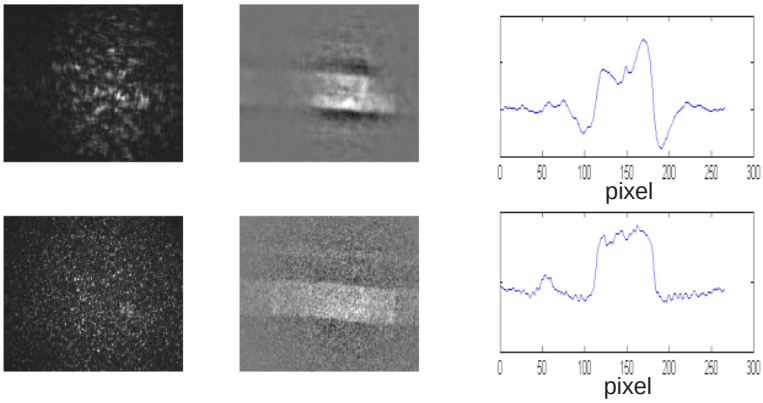

Figure 5: Influence of the constant phase area displayed in the LCTV. Top, the area occupies 6x6 pixels, bottom 1x1 pixel

It is clearly visible that the ghost image gets worse when using bigger area sizes of constant phase on the LCTV.

In ghost imaging experiments it is relevant to know how many measurements should be done in order to obtain a good quality image, i.e. how fast the process converges. To this end we have implemented the ghost imaging process by using an increasing amount of measurements ranging from 2000 to 20000. As an example figure 6 shows some of the results achieved for different amount of measurements and that corresponding to the slit under direct laser illumination.

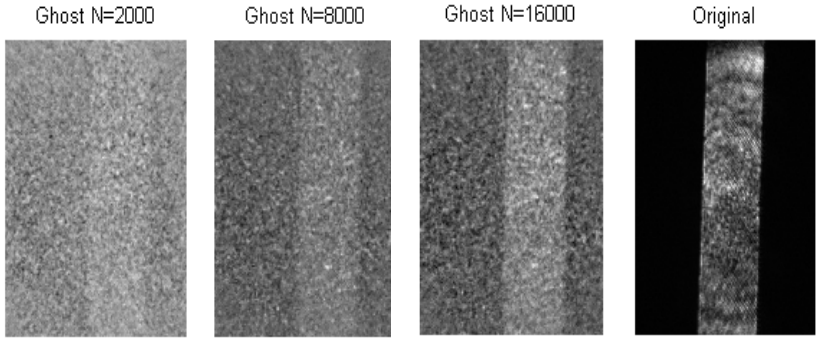

Figure 6: Ghost images obtained by increasing the amount of measurements

It is apparent that after 8000 measurements the result is practically the same.

3.2. Ghost diffraction

In order to implement the far field (Fraunhofer) ghost diffraction process we have mounted the set up described at the beginning of this Section, where lens L_3 was removed. In this case the CCD plane is the Fourier transform of the object plane and the ghost diffraction pattern is obtained by applying the process mathematically described in equation (3). We have used double slits as objects in these experiments. Figure 7a) shows the classical interference pattern that is obtained when a direct laser

beam illuminates the two slits. After introducing a random phase distribution, by means of the SLM, an image grabbed in the object arm is shown in the top right corner. As now the source is spatially incoherent, the Fourier transform of the object is not observable. The image corresponding to the reference arm is displayed in the bottom left. The ghost far field distribution obtained after 1000 phase realizations is shown in the bottom right corner.

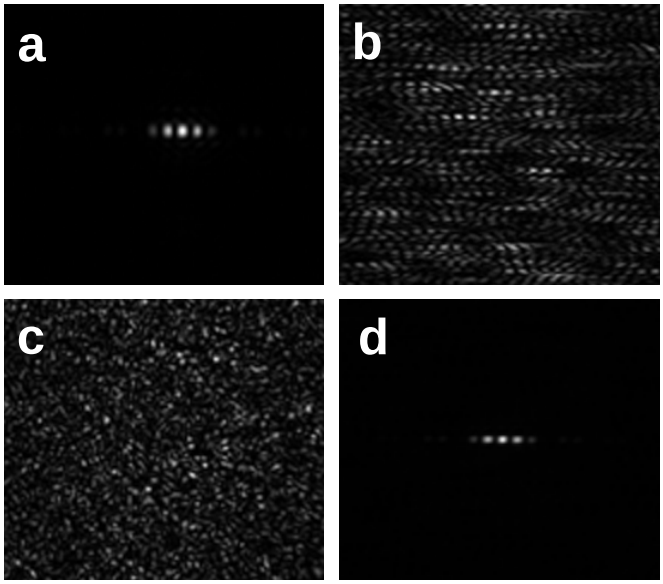

Figure 7: Ghost diffraction. a) Fraunhofer pattern generated by the object under direct laser illumination, b) an image of the object arm when a random phase distribution is displayed on the SLM, c) idem in the reference arm, d) ghost far field distribution after 1000 phase realizations

In figure 8a) it is shown the intensity profile of the interference pattern obtained under direct laser illumination, in figure 8b) it is depicted the profile corresponding to the far field ghost pattern.

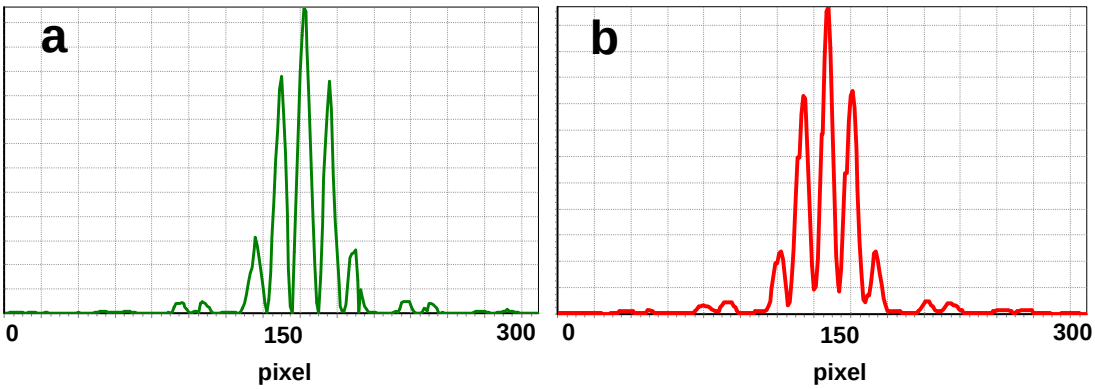

Figure 8: Intensity profiles corresponding to a) interference pattern shown in figure 7a); b) the ghost far field distribution shown in figure 7b).

It is noticeable that this distribution is accurately reconstructed after only 1000 phase realizations. This fast convergence is because the spatial cross correlation of the intensities is calculated as a function

of the displacement $\vec{x}_2 - \vec{x}_1$ between the pixel positions in the two arms, and by making an additional average over pixel positions at each fixed $\vec{x}_2 - \vec{x}_1$as explained in Section 2. Unfortunately this procedure cannot be applied in ghost imaging.

4. Conclusions

In this work we have implemented the use of a programmable phase spatial light modulator in order to produce pseudo-thermal beams which allow to perform correlated imaging processes. The highly spatial correlated speckle beams obtained from the random phase distributions displayed in the LCTV emulate those produced with a moving diffuser but with the advantage that the process is entirely programmable and the speckle distributions are easily controllable. Based on this feature we have analyzed the influence of the speckle size, phase distributions and convergence rate on the correlated image quality. Two different cases have been carried on, ghost imaging and far field ghost diffraction.

Acknowledgments

This research was supported by Universidad de Buenos Aires X118, X103, ANPCyT PICT 2284 and CONICET PIP 3047, Argentina.

References

[1] Ribeiro P, Padua S, Machado da Silva J and Barbosa G 1994 *Phys. Rev. A* **49** 4176
[2] Strekalov D, Sergienko A, Klyshko D and Shih Y 1995 *Phys. Rev. Lett.* **74** 3600
[3] Pittman T, Shih Y, Strekalov D and Sergienko A 1995 *Phys. Rev. A* **52** R3429
[4] Abouraddy A, Saleh B, Sergienko A and Teich M 2001 *Phys. Rev. Lett.* **87** 123602
[5] Bennink R, Bentley S and Boyd R 2002 *Phys. Rev. Lett.* **89** 113601
[6] Gatti A, Brambilla E, Bache M and Lugiato L 2004 *Phys. Rev. Lett.* **93** 093602
[7] Ferri F, Magatti D, Gatti A, Bache M, Brambilla E and Lugiato L 2005 *Phys. Rev. Let.* **94** 183602
[8] Gatti A, Brambilla E, Bache M and Lugiato L 2004 *Phys. Rev. A.* **70** 013802
[9] Bennink R, Bentley S and Boyd R 2004 *Phys. Rev. Lett.* **92** 033601
[10] Erkmen B and Shapiro J 2008 *Phys. Rev. A.* **77** 043809
[11] Scarcelli G, Berardi V and Shih Y 2006 *Phys. Rev. Lett.* **98** 063602
[12] Shapiro J 2008 *Phys. Rev. A.* **78** 061802(R)
[13] Bache M, Brambilla E, Gatti A and Lugiato L 2004 *Opt. Exp.* **12** 6067
[14] Marquez A, Iemmi C, Moreno I, Davis J, Campos J and Yzuel M 2001 *Opt. Eng.* **40** 2558